

1,4-Diurea- and 1,4-Dithiourea-Substituted Aromatic Derivatives Selectively Inhibit α -Synuclein Oligomer Formation *In Vitro*

Susantha K. Ganegamage, Eduardo Ramirez, Heba Alnakhala, Arati Tripathi, Cuong Calvin Duc Nguyen, Ashique Zami, Raluca Ostafe, Shiliang Tian, Ulf Dettmer, and Jessica S. Fortin*



Cite This: *ACS Omega* 2024, 9, 1216–1229



Read Online

ACCESS |



Metrics & More

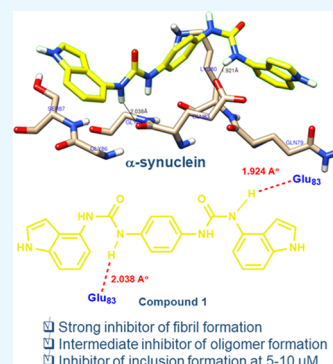


Article Recommendations



Supporting Information

ABSTRACT: Parkinson's disease (PD) is the second most common neurodegenerative disease, affecting the elderly population worldwide. In PD, the misfolding of α -synuclein (α -syn) results in the formation of inclusions referred to as Lewy bodies (LB) in midbrain neurons of the substantia nigra and other specific brain localizations, which is associated with neurodegeneration. There are no approved strategies to reduce the formation of LB in the neurons of patients with PD. Our drug discovery program focuses on the synthesis of urea and thiourea compounds coupled with aminoindole moieties to abrogate α -syn aggregation and to slow down the progression of PD. We synthesized several urea and thiourea analogues with a central 1,4-phenyl diurea/thiourea linkage and evaluated their effectiveness in reducing α -syn aggregation with a special focus on the selective inhibition of oligomer formation among other proteins. We utilized biophysical methods such as thioflavin T (ThT) fluorescence assays, transmission electron microscopy (TEM), photoinduced cross-linking of unmodified proteins (PICUP), as well as M17D intracellular inclusion cell-based assays to evaluate the antiaggregation properties and cellular protection of our best compounds. Our results identified compound **1** as the best compound in reducing α -syn fibril formation via ThT assays. The antioligomer formation of compound **1** was subsequently superseded by compound **2**. Both compounds selectively curtailed the oligomer formation of α -syn but not tau 4R isoforms (0N4R, 2N4R) or p-tau (isoform 1N4R). Compounds **1** and **2** failed to abrogate tau 0N3R fibril formation by ThT and atomic force microscopy. Compound **2** was best at reducing the formation of recombinant α -syn fibrils by TEM. In contrast to compound **2**, compound **1** reduced the formation of α -syn inclusions in M17D neuroblastoma cells in a dose-dependent manner. Compound **1** may provide molecular scaffolds for the optimization of symmetric molecules for its α -syn antiaggregation activity with potential therapeutic applications and development of small molecules in PD.



INTRODUCTION

Parkinson's disease (PD) is a multifactorial chronic neurodegenerative disease that affects 10 million people worldwide and currently approximately 1 million Americans.¹ One important player in the pathophysiology of PD are Lewy bodies (LB), which consist of large inclusions found in the neurons located in the nuclei of the midbrain responsible for the control of fine motor movement.² These inclusions are generated from misfolding and accumulation of α -synuclein (α -syn), a protein involved in neuronal transmission.³ The involvement of LB in neurodegeneration is well established, but a detailed understanding of their involvement in pathophysiology is missing.⁴ It has been suggested that LBs might be rather inert, while smaller aggregates are more pathogenic. Among those, the formation of oligomers may be the toxic moiety rather than the larger fibrils generated from misfolded α -syn.⁵ Many studies are focused on understanding the spreading of the misfolded α -syn which seems to be a major event taking place in the pathophysiology of PD. Currently, FDA-approved drugs are alleviating the symptoms, but there are no small-molecule therapeutics available to reduce or delay the formation of LB.

Several other researchers have been working on the discovery of small molecular scaffolds based on sulfonyls,⁶ sulfonamides,^{7,8} triazoles,⁹ thiadiazoles,¹⁰ ureas,^{11,12} amines,^{13,14} or aminoindoles,^{12,14} to impede the formation of oligomers. Urea is a stable hydrophilic functional moiety that is used to convert and store nitrogenous waste in the terrestrial animal body as a metabolic byproduct until excreted.¹⁵ The biological activity of urea has not been fully investigated.¹⁵ However, some researchers have proven that urea and thiourea can interact with proteins to inhibit their aggregation.^{11,12,16,17} They have specifically demonstrated a chaotropic effect via disintegrating inter- and intramolecular noncovalent interactions.¹⁸

Prior published work from our lab described the antiaggregation properties of aminoindole, and we pursued the exploration of new molecules using this building block to design

Received: September 26, 2023

Revised: November 28, 2023

Accepted: November 30, 2023

Published: December 19, 2023



a new family of antiaggregation compounds, with a special focus on antioligomer properties.¹⁴ The effects of urea- and thiourea-based compounds on α -syn oligomer and fibril formation have not been explored. In this study, we prepared a series of aminoindole-derived diurea and dithiourea bioisosteric analogues to evaluate and compare their effects on α -syn misfolding and aggregation using thioflavin T (ThT) fluorescence assays, transmission electron microscopy (TEM), photoinduced cross-linking of unmodified proteins (PICUP), and circular dichroism (CD). The cytoprotection and anti-inclusion effect conferred by the best compounds were assessed using the M17D intracellular inclusion cell-based assay. We also examined if the antioligomer effect is specific (i.e., only affecting one protein, such as α -syn) or general (i.e., can be applied to other protein such as tau and hyperphosphorylated tau (p-tau)).

RESULTS AND DISCUSSION

Chemistry. We selected aminoindoles as the main substituents of the 1,4-diurea and 1,4-dithiourea analogues based on their antioligomer activity demonstrated by the PICUP assay (Figure 1). The syntheses of diurea (1, 3, 5, 7, and 9) and

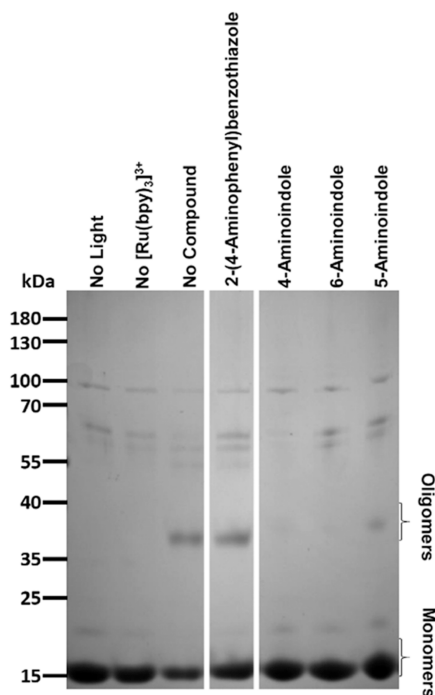


Figure 1. Aminoindoles inhibited α -syn oligomer formation by PICUP. α -Syn ($60 \mu\text{M}$) was cross-linked (PICUP assay) with DMSO (control) or the compound at $50 \mu\text{M}$ (\sim molar ratio, 1:1). 4-, 5-, 6-Aminoindoles, but not the 2-(4-aminophenyl)benzothiazole,¹³ abrogated the formation of high molecular bands (i.e., oligomers) visible between 35 and 40 kDa. Coomassie blue-stained polyacrylamide gels showed high-molecular-weight α -syn oligomers with the control (0.125% DMSO). Additional controls consist of no light exposure and no cross-linking agent (no Ru(bpy)), which provided no cross-linked products.

its bioisosteric dithiourea analogues (2, 4, 6, 8, and 10) are shown in Scheme 1. The synthesis of analogues was achieved via the nucleophilic addition of corresponding amines (a–e in Table 1), mainly four aminoindoles and one aniline, with respective diisocyanate (P) or diisothiocyanate (Q) shown in Table 1 and Scheme 1. All of the analogues have a topological polar surface area (TPSA) in the range of 79–114 Å² with <4

hydrogen-bond donors (HBD), which successfully adheres to Lipinski's rule.

Compound 1, a Diurea Derivative, Exhibits the Best α -Syn Antifibril Activity as Monitored by the Thioflavin-T (ThT) Fluorescence Assay. We explored the thematic of symmetric molecules based on our previous work on urea^{11,12} and amide¹⁴ compounds using aminoindolyl groups and their antioligomer properties (Figure 1). The impact of different positions of the aminoindolyl group linked molecules on the kinetics of α -syn fibril formation was assessed using thioflavin T (ThT) assays by measuring the percentage of fluorescence intensities (FI). The FIs of the newly synthesized compounds were compared with the control (DMSO), and the reduction of the percentage FI to 15% or less was considered as the cutoff value to move the compound to tier-2 assays. Based on the data obtained for the 10 derivatives (i.e., compounds 1–10), 4-aminoindolyl derivatives (compounds 1–2) were greater inhibitors of α -syn fibril formation than the 5-, 6-, 7-aminoindolyl derivatives (compounds 3–8) (Table 1). In the case of all aminoindolyl groups (compounds 1–8), the 4-aminoindolyl group (compounds 1–2) was the most preferred substituent. The change of the aminoindolyl group for a simple aromatic moiety (compounds 9–10) led to complete loss of the α -syn antifibrillary activity.

Initial molecular docking results indicated that analogue 1 (−5.55) has a slightly higher binding with a hydrophobic binding pocket on the active site but analogue 2 is closer to the hydrophilic binding (−4.63) with strong hydrogen bonding with three different amino acid residues (Val77, Ala78, and Thr81), which might stabilize the ligand-protein/receptor interaction (Table S3) (Figure 2).^{19,20} More stable ligand–receptor complexes can exhibit higher activity in the dynamic biological system.²¹

The kinetics of α -syn fibril formation following treatment with $100 \mu\text{M}$ compounds 1 and 2 are shown in Figure 3A. Compound 1 and 2 delayed the lag time in comparison to the control (DMSO treatment). Based on the initial ThT and molecular docking results (and biological activity shown later), the dose–response curve was obtained only for compounds 1 and 2 (Figure 3). The resulting Log(agonist) vs normalized response (variable slope) correlation obtained by Prism provided a LogEC50 of 19.7 ± 2.1 and 29.5 ± 5.3 for compounds 1 and 2, respectively. The curve shows a dose-dependent linear response not related to the solubility of compounds as the fibril reduction has been confirmed by TEM. In addition, the dose dependency has been demonstrated with cell-based assays at low micromolar concentrations.

Compounds 1 and 2 Did Not Substantially Abrogate Tau ON3R Fibril Formation. The antifibrillary effects of compounds 1 and 2 were examined on tau isoform ON3R using, ThT assay (Figure 4). Both compounds were not effective at disrupting the aggregation propensity of tau ON3R. After 18 h, the percent decreases were −18.1 and 30.5 for compounds 1 and 2, respectively. Compound 1 increased the ThT fluorescence intensity, indicative of an elevated amount of fibrils in comparison to the nontreated control. Compound 2 exhibited a weak antifibrillar effect on tau isoform ON3R.

Atomic force microscopy (AFM) was performed after 47 h (Figure 5) and the resulting fibrils were measured in terms of length and height (Table 2). AFM fibril measurements aligned well with the ThT findings. High magnifications showed abundant fibrils in tau samples supplemented with compound 1 or 2 in comparison with the nontreated control. In addition to

Scheme 1. Preparation of 1,4-Diurea (1, 3, 5, 7, 9) and 1,4-Dithiourea Compounds (2, 4, 6, 8, 10) Using the Relevant Aromatic (Ar) Amines (a–e) and Diisocyanates (P) or Diisothiocyanate (Q) to Generate the Final Products Presented in Table 1

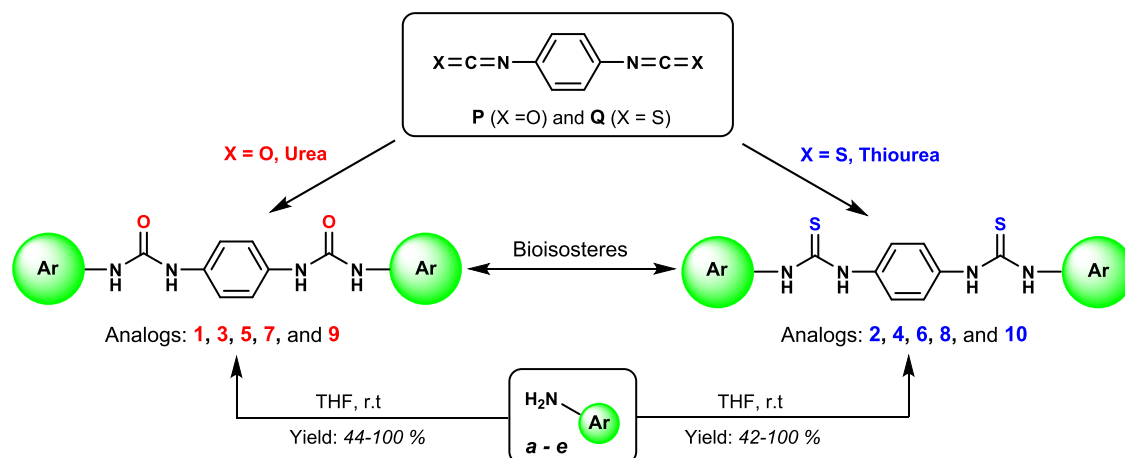


Table 1. Molecular Structures of Novel Diurea- and Dithiourea-linked Derivatives and Their Respective Antifibrillary Activity on α -Synuclein (α -Syn, 6 μ M Final Concentration) Expressed as Maximum Thioflavin T (ThT) Intensity in Percentage in Which the Compounds Were Tested at 100 μ M^a

Amines (a–e)	Diisocyanate /Diisothiocyanate P (X = O) Q (X = S)	Functional Groups A		
			X = O, Urea	X = S, Thiourea
	 P or Q		1 10.1 ± 2.0	2 18.9 ± 2.3
			3 71.1 ± 6.1	4 68.9 ± 4.2
			5 68.5 ± 4.4	6 41.8 ± 2.5
			7 80.0 ± 8.0	8 61.5 ± 6.2
			9 94.2 ± 4.1	10 82.3 ± 4.5

^aData represents the average of three replicates with standard error of the mean (SEM).

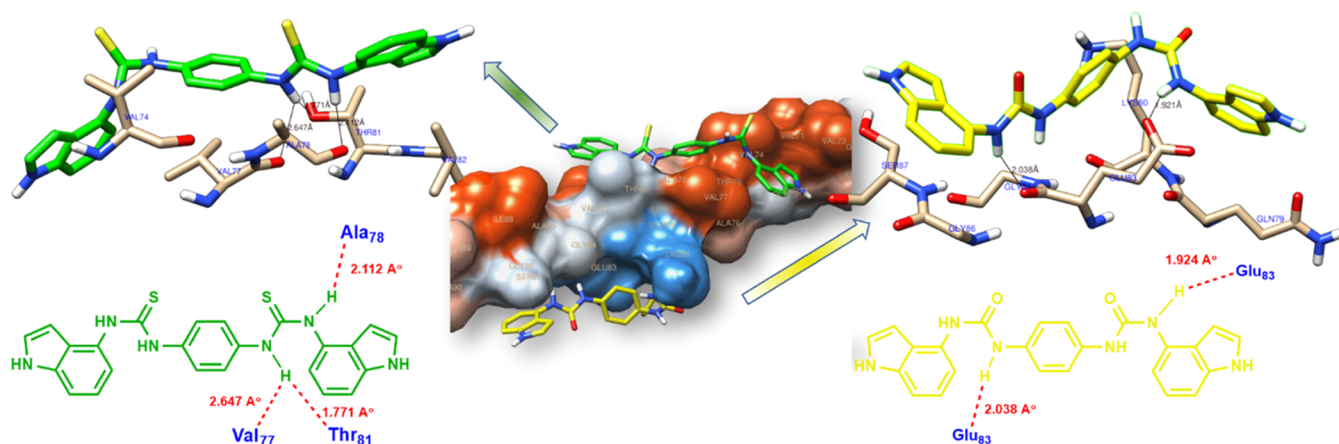


Figure 2. Docking of analogue 2 (green color on left) and 1 (yellow color on right) and their binding locations on human α -syn protein (PDB ID: 1XQ8) within the active site (middle) with hydrogen bonding.

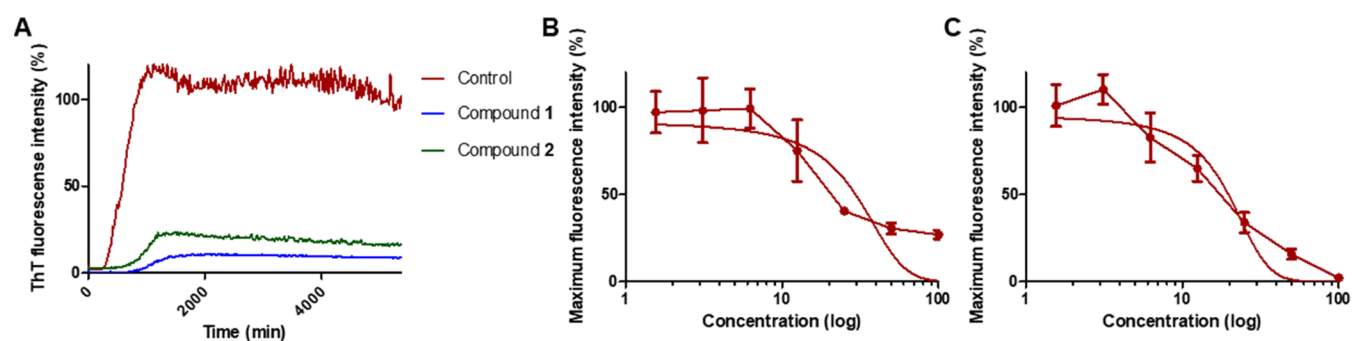


Figure 3. ThT kinetic curves (A) and dose-dependent reduction of α -synuclein (α -syn) fibrillation by compound 1 (B) and compound 2 (C). (A) Kinetic curves were achieved using 100 μ M compounds 1 and 2. The control consisted of the vehicle (DMSO at 0.25%). (B, C) Dose-dependent curves resulted from incubations carried out with α -syn at 47 h with four concentrations (i.e., 12.5, 25, 50, and 100 μ M) of the best α -syn antifibrillary compounds 1 and 2 of the diurea/dithiurea analogues. Triplicate data were collected from 10 consecutive time points at the plateau phase. For both experiments, α -syn was tested at 6 μ M.

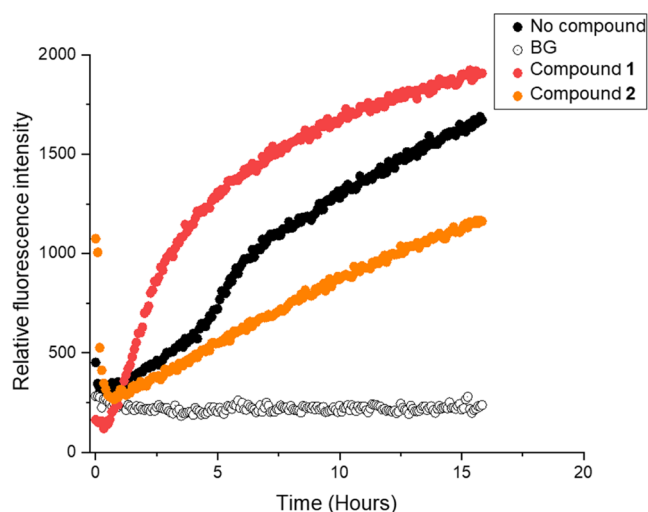


Figure 4. Kinetics of tau 0N3R fibril formation: comparison of compounds 1–2 and control (no compound) monitored using thioflavin T (ThT) fluorescence assays. Compounds were tested at a final concentration of 100 μ M in the presence of 10 μ M Tau 0N3R, 2.5 μ M heparin, 1 mM dithiothreitol (DTT), 1 mM 4-(2-aminoethyl)benzenesulfonyl fluoride hydrochloride, and 30 μ M ThT in a CHELEX-treated buffer consisting of 50 mM Tris, 25 mM NaCl, pH 7.4. The molar ratio of protein:compound was 1:10. The positive control consisted of Tau 0N3R without compound treatment. The background (BG) signal was obtained with all components in the absence of heparin.

inducing formation of fibrils, compound 1 increased the length and height of the tau 0N3R fibrils in comparison to the nontreated control. Compound 2 demonstrated a very weak antifibrillary effect. Interestingly, measurements showed a modest reduction in the fibril length versus the control without an effect on the tau 0N3R fibril height.

Compounds 1 and 2 Exhibit an Antioligomer Activity on α -Synuclein but Not Tau (Isoform 0N4R) and p-Tau (Isoform 1N4R). PICUP is a technique utilized to analyze high-molecular-weight cross-linked proteins reflective of oligomer formation. Figure 6 shows α -syn high-molecular-weight oligomeric species detected at around 37 and 55 kDa in the Coomassie blue-stained 16% polyacrylamide gel. DMSO treatment resulted in a high-molecular-weight band around 37 kDa. The sample not exposed to light or cross-linking agent demonstrated a prominent monomeric band at 15 kDa. The

relative pixel density (RPD) of the DMSO condition has been compared with the RPD of each representative treatment. A RPD below 2.85 (i.e., $\geq 50\%$ reduction of oligomer formation) was considered as the cutoff. Compounds 8, 2, and 1 reduced the formation of α -syn oligomers, with respective percentages of oligomer reduction of 91.2, 84.2, and 52.6%. Compounds 3, 4, 5, and 6 demonstrated mediocre α -syn antioligomer effects by PICUP.

Another PICUP experiment was performed to confirm that compound 2 exhibits a dose-dependent antioligomer activity. Lower concentrations of α -syn were utilized in order to study the low micromolar concentration of compound 2. The latter exerted a strong α -syn antioligomer activity at a molar ratio 1:1 (Figure 7). The antioligomer activity was moderately (not fully) effective at 7.5 μ M. At 15 μ M, bands occurred between 40 and 60 kDa representing higher-molecular-weight oligomers. They are markedly reduced compared to the bands resulting from the control condition (DMSO treatment at 0.125%).

Previous work on dual antiaggregation effects of compounds on α -syn and tau performed in our lab^{7,13,14} spurred the investigation of additional compounds for their antioligomer activity on tau isoform 0N4R (Figure 8), tau isoform 2N4R (Figure 9), and p-tau isoform 1N4R (Figure 10). PICUP experiments were performed with compounds 1 and 2. Compounds 1 and 2 are disubstituted with a 4-aminoindolyl. Compound 1 represents the urea counterpart of compound 2. None of these compounds was able to reduce the tau 0N4R (Figure 8) and 2N4R (Figure 9) oligomer formation by PICUP. p-Tau isoform 1N4R was challenged with compounds 1 and 2 using the PICUP assays. The best α -syn antifibrillary compounds failed to inhibit p-tau oligomer formation (Figure 10). We next proceeded with the TEM analysis of α -syn fibrils subjected to the best compound treatments.

Compounds 1 and 2 Reduced the Formation of α -Syn Fibrils. To confirm the general antifibrillar effect of the best inhibitor of fibril formation, i.e., compounds 1 and 2, TEM was utilized as a direct means to detect α -syn fibrils. Samples were collected at the end of the ThT kinetics of aggregation to visualize fibrils and to compare the effects of compound 1 or 2 with those of DMSO. Compounds and α -syn were tested at 100 and 2 μ M, respectively. Figure 11 shows the photomicrographs acquired at 40K magnification. Application of α -syn resulted in a very dense mat of fibrils at the end of the kinetics of fibril formation (~ 22 h at 37 $^{\circ}$ C). Both compounds 1 and 2 reduced α -syn fibril formation in comparison to controls (1.5% DMSO).

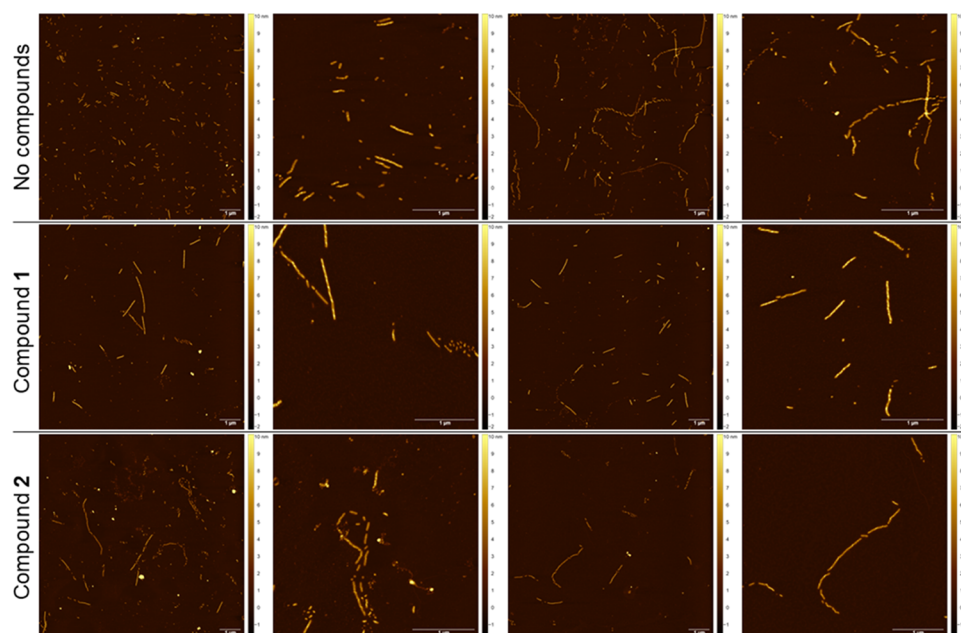


Figure 5. Compounds 1 and 2 failed to reduce tau 0N3R fibril formation as validated by atomic force microscopy (AFM). Tau isoform 0N3R (10 μM) was incubated with no treatment, compound 1 (100 μM), or compound 2 (100 μM) for 47 h prior to AFM visualization (molar ratio 1:10). Images were collected at sizes of $10 \times 10 \mu\text{m}^2$ and $3.33 \times 3.33 \mu\text{m}^2$. Scale bars located at the bottom right corner are 1 μm .

Table 2. Average Numbers of Tau 0N3R Fibrils Sharing the Same Contour Length (L , nm) and Average Height (h , nm) for Each Condition, i.e., No Compound, Compound 1 (100 μM), and Compound 2 (100 μM)^a

AFM analyses	length (nm)	height (nm)
no compound	268.26 ± 115.73	5.40 ± 1.16
compound 1	409.01 ± 300.11	7.50 ± 0.85
compound 2	219.40 ± 166.36	5.97 ± 0.87

^a10 μM tau 0N3R was incubated in the absence or presence of compound for 47 h.

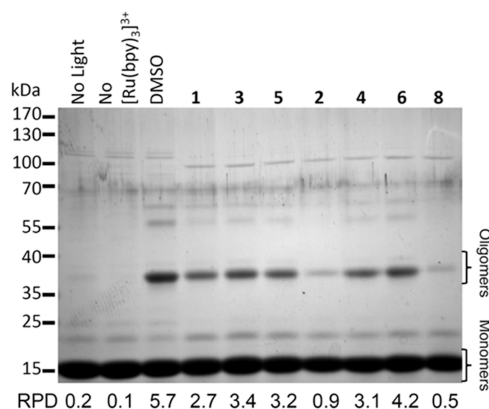


Figure 6. Compounds 1, 2, and 8 reduced the level of α -syn oligomer formation by PICUP. α -Syn (60 μM) was cross-linked (PICUP assay) with DMSO (control) or compound at 50 μM (\sim molar ratio, 1:1). Compounds 3, 4, 5, and 6 slightly reduced the formation of high molecular bands (i.e., oligomers). The pixel density of the high-molecular-weight bands labeled as oligomers and the low molecular bands identified as monomers have been quantified by image J. The relative pixel density (RPD) was obtained by dividing the pixel density of the higher molecular bands for each condition by their respective monomeric band.

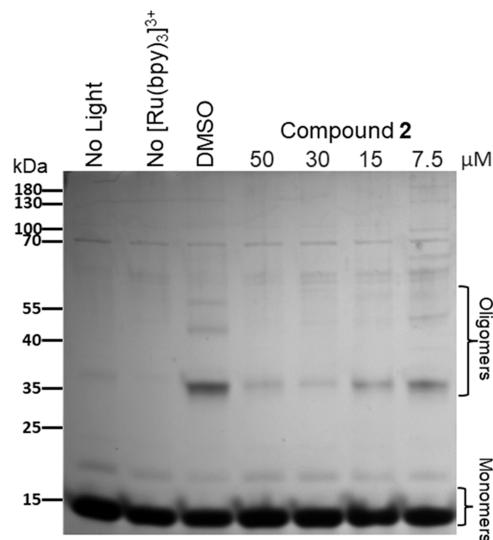


Figure 7. Evidence of the dose-dependent inhibitory activity of compound 2 on α -syn oligomerization determined using the PICUP assay. The protein (30 μM) was incubated with compound 2: 50 μM (molar ratio 1:1.6), 30 μM (molar ratio 1:1), 15 μM (molar ratio 1:0.5), and 7.5 μM (molar ratio 1:0.25). The inhibition of α -syn oligomerization by compound 2 is dose-dependent. The control consisted of DMSO (0.125%).

Fibrils were also shorter in α -syn samples treated with compounds 1 and 2.

Compounds 1 and 2 Reduced the Conversion to α -Syn β -Sheet Conformation. Far-UV circular dichroism (CD) spectra were recorded to provide structural information after treatment of α -syn (at 12 μM) with 100 μM compounds 1 and 2 for 0, 24, and 48 h at 37 $^\circ\text{C}$ (Figures 12 and 13). Both compounds 1 and 2 substantially reduced the intensity of the peak at 225 nm corresponding to a β -sheet conformation at 48 h (Figure 13). Curcumin did not delay the conversion to α -syn β -

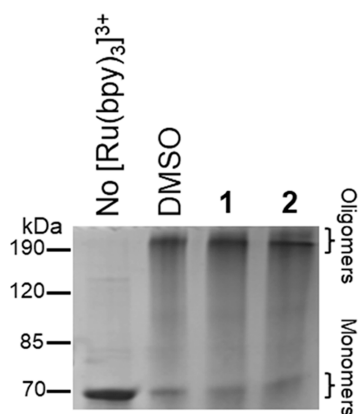


Figure 8. 1,4-Diurea- and dithiourea-substituted aromatic representatives failed to inhibit tau 0N4R oligomer formation by PICUP. Compounds 1 and 2 were selected for their α -syn antioligomerization activity. Tau 0N4R ($6 \mu\text{M}$) was cross-linked (PICUP assay) with the disubstituted aminoindolyl derivatives at $50 \mu\text{M}$ (\sim molar ratio, 1:8).

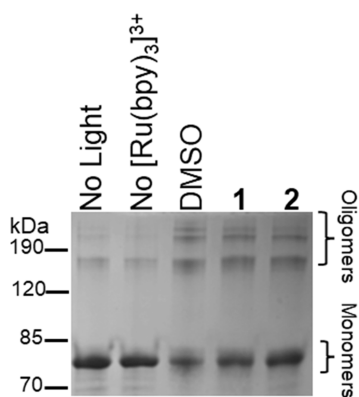


Figure 9. Compounds 1 and 2 did not inhibit tau isoform 2N4R oligomer formation. Tau 2N4R ($6 \mu\text{M}$) was cross-linked (PICUP assay) with different compounds at $50 \mu\text{M}$ (\sim molar ratio, 1:8). Coomassie blue-stained polyacrylamide gels showed high-molecular-weight tau oligomers with control (0.125% DMSO; lane 3) as well as compounds 1 and 2.

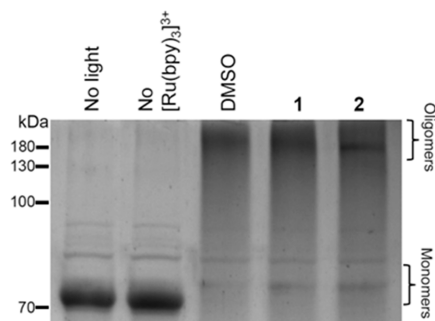


Figure 10. 1,4-Diurea- and dithiourea-substituted aromatic representatives did not prevent p-tau 1N4R oligomer formation by PICUP. p-Tau isoform 1N4R ($6 \mu\text{M}$) was cross-linked (PICUP assay) with $50 \mu\text{M}$ compounds 1 and 2 (molar ratio \sim 1:8).

sheet formation. Trend was reproduced with a commercial source of the protein.

Compound 2 Disaggregates Recombinant α -Syn Fibrils *In Vitro*. α -Syn fibrils were generated (preformed) in order to evaluate the disaggregation effects of compounds 1 and 2. The experimental conditions used for regular α -syn ThT were

applied with the exception that the diluted protein solution was preincubated for 48 h in 10 mM PBS (pH 7.4), supplemented with 0.5 mM SDS and 300 mM NaCl. The fluorescence signal decreased and reached a plateau phase for about 40 h. After a period of 40 h, the ThT assay was processed and samples were collected to visualize fibrils and to compare the effects of the compounds. The maximum fluorescence intensity values were significantly reduced in the presence of compounds 1 and 2, indicative of disaggregation (Figure 14A). TEM analyses confirmed the presence of fewer and shorter fibrils for the mature fibrils subjected to compound 1 and 2 treatment (Figure 14B)

Compound 1 Reduces α -Syn Inclusion in Neuroblastoma Cells. The established dox-inducible neuroblastoma M17D-TR/ α S3K::YFP cell-based assay was selected to evaluate the effect of compounds in preventing inclusion formation following induction with Dox.^{7,22,23} Compound 8 demonstrated a weak effect on fibril formation and an inhibitory effect on oligomerization. Treatment of cells with compound 8 resulted in very minimal changes in the number of inclusions at various concentrations from 1.25 to $10 \mu\text{M}$ (Figure 15). By contrast, compound 1 reduced α -syn inclusion formation at 5 and $10 \mu\text{M}$, with the most significant decreases occurring at low micromolar concentrations ($10 \mu\text{M}$). Compound 2, which demonstrated a prominent antioligomer effect, increased the inclusions at 5 and $10 \mu\text{M}$. Compounds 1, 2, and 8 did not result in changes in the cell confluence.

CONCLUSIONS

We evaluated 10 diurea/dithiourea compounds with a 1,4-phenyl diurea/thiourea linkage for their antiaggregation properties against α -syn aggregation. In order to characterize such antifibrillary activity, ThT fluorescence assays and transmission TEM were utilized. The antioligomer activity of the best compounds was assessed with several prone-to-aggregate proteins by PICUP. Afterward, the biological effect of the best compounds was studied using the M17D intracellular inclusion cell-based model. Based on the antifibrillary biophysical assays, compounds 1 and 2 (a 1,4-phenyl urea or thiourea with two 4-aminoindolyls) were identified as the most promising lead molecules in the series of compounds presented in this manuscript. Compounds 2 and 8, and to a lesser extent compound 1, were effective in reducing α -syn oligomer formation but not tau (isoforms 0N4R and 2N4R) and p-tau isoform 1N4R. In addition, compounds 1 and 2 failed to inhibit tau 0N3R fibril formation by ThT and AFM analyses. Interestingly, our cell-based studies showed no α -syn anti-inclusion effect of compound 8, which exhibited a modest α -syn antifibrillar and greatest α -syn antioligomer effects. A significant reduction in the number of M17D α -syn inclusions was detected following compound 1 treatment at a low micromolar concentration. The opposite effect, i.e., an increase in α -syn inclusion, in cells treated with compound 2 using the same concentration ($10 \mu\text{M}$). Importantly, no changes in confluence with compounds 1, 2, and 8 were noticed. Thus, compound 2 failed to prevent α -syn inclusions in a cell-based model while compound 1 was effective in reducing inclusions, while neither of the two compounds displayed cytotoxic effects. This study was performed to provide insight into antifibrillar, antioligomer, and anti-inclusion effects of symmetric molecules specific to 1,4-diurea-phenyl- and 1,4-dithiourea-phenyl-substituted with aminoindolyl, with the 4-aminoindolyl resulting in the best

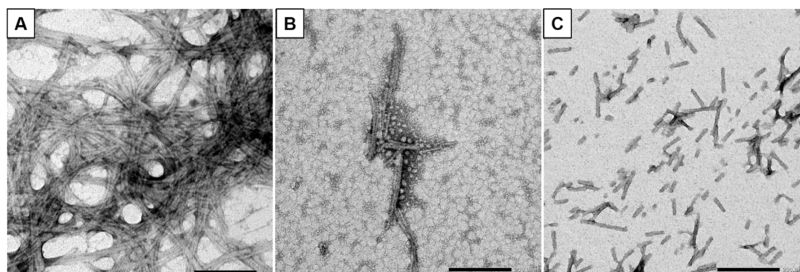


Figure 11. Compound 1 and 2 treatments resulted in fewer and shorter α -synuclein (α -syn) fibrils by transmission electron microscopy (TEM). (A) α -Syn ($2 \mu\text{M}$) was incubated with DMSO (0.25%; 'CTRL'); (B) α -Syn ($2 \mu\text{M}$) was treated with compound 1 at $100 \mu\text{M}$; (C) α -Syn ($2 \mu\text{M}$) was subjected to compound 2 treatment at $100 \mu\text{M}$. Incubation time was ~ 22 h prior to TEM visualization. Scale bars = 200 nm.

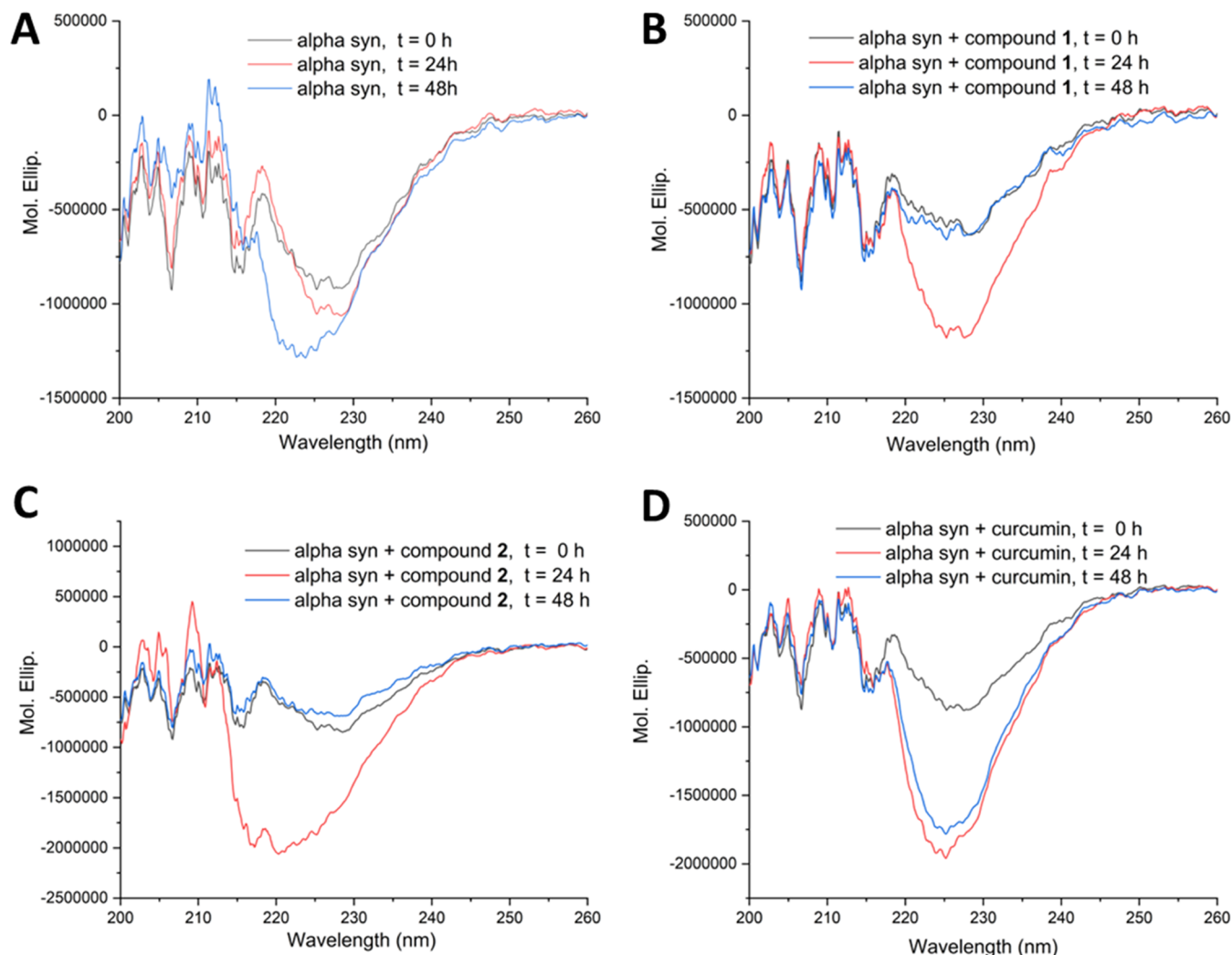


Figure 12. CD spectra of α -syn incubated at different time points in the absence and presence of compounds. (A) CD spectra of α -syn are characteristic of unfolded, random coils with slight formation β -sheet at time 0 h and show conversion to α helix and additional β -sheet conformation at 48 h. (B, C) Treatment with $100 \mu\text{M}$ compounds 1 and 2 converted the protein to random coils with fewer β -sheet conformation at 48h. (D) Curcumin treatment did not demonstrate such structural changes.

biophysical and biological activities based on the assays performed.

EXPERIMENTAL SECTION

General Characterizations. ^1H and $^{13}\text{C}\{^1\text{H}\}$ NMR spectra were recorded using a 500 MHz Bruker instrument working at a frequency of 500 MHz for ^1H and at 126 MHz for ^{13}C . Chemical shifts are reported in ppm using residual solvent resonances as

internal reference (δ 2.50 and δ 39.51 for ^1H and ^{13}C in $\text{DMSO}-d_6$, respectively). ^1H NMR data are reported as follows: b = broad, s = singlet, d = doublet, t = triplet, q = quartet, and m = multiplet. Coupling constants are given in hertz. The purity of all compounds and synthetic intermediates was judged to be 95% or better based on ^1H NMR. IR measurements were performed in a Nicolet FTIR instrument as thin films in the Purdue Drug

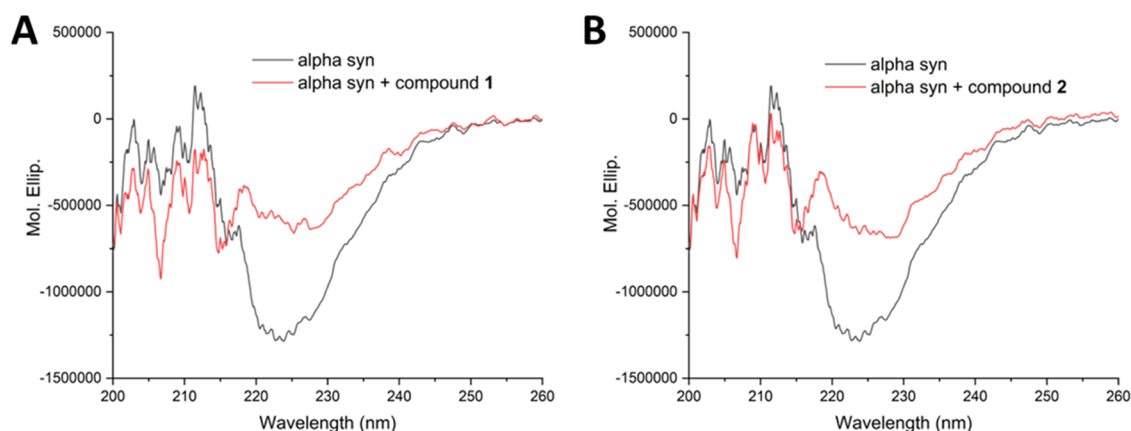


Figure 13. Compounds **1** and **2** reduced the amount of α -syn α helix intermediate and β -sheet conformation after incubation of 48 h at 37 °C. (A) CD spectra of α -syn were incubated with 100 μ M compound **1**. (B) CD spectra of α -syn treated with 100 μ M compound **2**. Protein was tested at 12 μ M in 10 mM PBS (pH 7.4) containing 300 mM NaCl and 0.5 mM SDS.

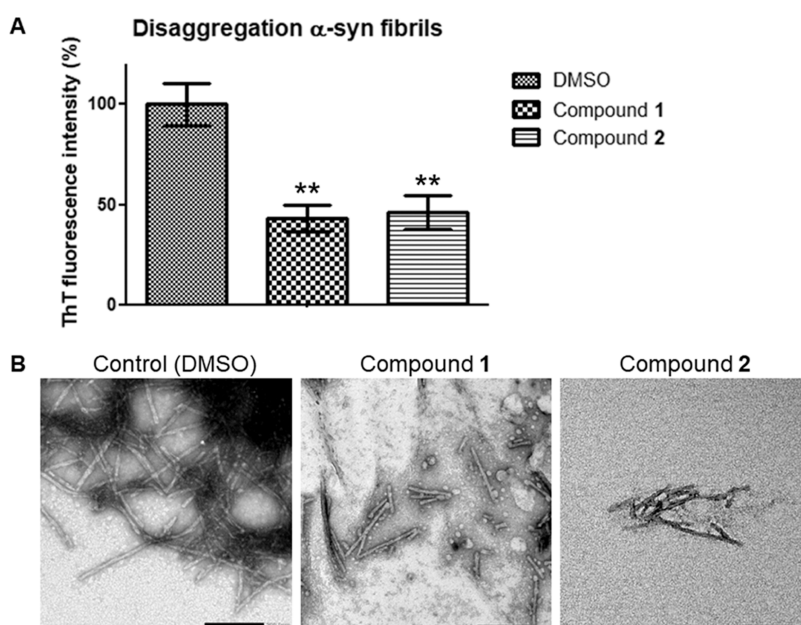


Figure 14. Compounds **1** and **2** disaggregate mature α -syn fibrils by ThT and TEM analyses. α -Syn was incubated at 37 °C at a concentration of 9.4 μ M in 10 mM PBS (pH 7.4), supplemented with 0.5 mM SDS and 300 mM NaCl for 48 h prior to any assays to allow the formation of mature fibrils. (A) Subsequently, a ThT experiment was performed using standard procedure, i.e., 6 μ M protein, 100 μ M compounds (including 3–6 replicates). At 40 h, the relative fluorescence intensity values were averaged and data were plotted using GraphPad Prism. Statistical analyses were applied using the one-way ANOVA with Dunnett's post hoc test; **, $p < 0.01$. (B) Samples were deposited on copper grids and analyzed by TEM. Representative pictures are shown herein. The scale at the bottom right corner is 200 nm.

Discovery facility. High-resolution mass spectrometry analyses were conducted at the MSU Mass Spectrometry facility.

General Synthetic Procedure (1–10). Respective aromatic anilines **a–e** (2.0 equiv) were dissolved in THF at r.t. The reaction mixture was charged with a respective diisocyanate (**P**, 1.0 equiv) or diisothiocyanate (**Q**, 1.0 equiv) at r.t. The reaction mixture was stirred at r.t. until all of the starting materials were consumed which was monitored by TLC. The resultant precipitate was filtered and washed thoroughly with hexane:dichloromethane (1:1) until it removes all of the amine traces to produce pure respective diurea (**1**, **3**, **5**, **7**, **9**) or dithiurea (**2**, **4**, **6**, **8**, **10**) analogues.

3-(1H-Indol-4-yl)-1-(4-[[1H-indol-4-yl]carbamoyl]amino)phenyl)urea (1). White solid (452 mg, yield: quantitative), $R_f = 0.22$ (dichloromethane/MeOH = 95: 5). ^1H NMR (500 MHz, DMSO) δ 11.11 (s, 1H), 8.79 (s, 1H), 8.43 (s, 1H), 7.67 (dd, $J =$

7.5, 1.1 Hz, 1H), 7.44 (s, 2H), 7.31 (t, $J = 2.8$ Hz, 1H), 7.06–6.99 (m, 2H), 6.57 (s, 1H). $^{13}\text{C}\{^1\text{H}\}$ NMR (126 MHz, DMSO) δ : 152.6, 136.5, 134.1, 132.7, 124.0, 121.6, 118.8, 107.3, 105.7, 97.7. Mp < 355 °C. HRMS (ESI/Q-TOF) m/z : $[\text{M} + \text{H}]^+$ calcd for $\text{C}_{24}\text{H}_{20}\text{N}_6\text{O}_2$ 425.1728; Found 425.1729. IR (cm^{-1}) $\nu = 3607, 3315, 1668, 1624, 1559, 1506, 1407, 1301, 1229, 1201, 746, 721$.

3-(1H-Indol-4-yl)-1-(4-[[1H-indol-4-yl]carbamothioyl]-amino)phenyl)thiourea (2). Ash solid (286 mg, yield: 63%), $R_f = 0.44$ (dichloromethane/MeOH = 95: 5). ^1H NMR (500 MHz, DMSO) δ 11.20 (s, 2H), 9.77 (s, 2H), 9.52 (s, 2H), 7.35 (s, 4H), 7.34 (t, $J = 2.8$ Hz, 2H), 7.27 (dd, $J = 16.5, 7.8$ Hz, 4H), 7.07 (t, $J = 7.8$ Hz, 2H), 6.46 (s, 2H). $^{13}\text{C}\{^1\text{H}\}$ NMR (126 MHz, DMSO) δ : 179.1, 137.0, 136.1, 130.6, 125.0, 123.8, 122.9, 121.0, 114.6, 109.0, 99.1. Mp 197.2–202.4 °C. HRMS (ESI/Q-TOF) m/z : $[\text{M} + \text{H}]^+$ calcd for $\text{C}_{24}\text{H}_{20}\text{N}_6\text{S}_2$ 457.1271; Found 457.1278. IR

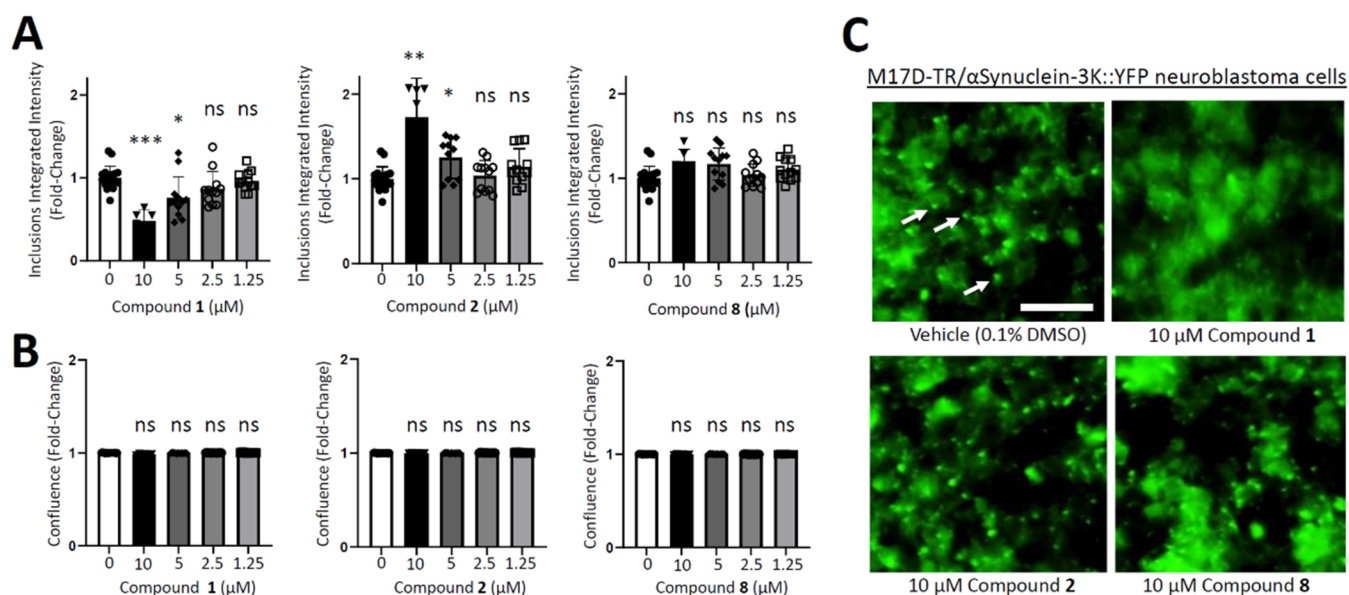


Figure 15. Compound 1 prevents α S inclusion formation. M17D cells expressing the inclusion-prone α S-3K::YFP fusion protein (dox-inducible) were treated with 0.1% DMSO (vehicle; “0 μ M”) as well as 1.25, 2.5, 5, and 10 μ M compounds 1, 2, and 8 at $t = 24$ h after plating. Cells were induced with doxycycline at 48 h. (A) IncuCyte-based analysis of punctate YFP signals relative to 0.1% DMSO was done at $t = 96$ h ($N = 3$) independent experiments, $n = 6$ –18 individual wells total (0 μ M, $n = 18$; 10 μ M, $n = 6$; all other concentrations, $n = 12$). (B) Same as (A), but confluence fold changes relative to DMSO vehicle (0 μ M) were plotted. (C) Representative IncuCyte images of reporter cells treated with vehicle versus 10 μ M compounds 1, 2, or 8 ($t = 96$ h), green channel. Arrows indicate α S-rich YFP-positive inclusions. Scale bar, 50 μ m. All data are presented as fold changes relative to DMSO control \pm standard deviation. One-way ANOVA, Dunnett’s post hoc test; *, $p < 0.05$; **, $p < 0.01$; ***, $p < 0.001$.

(cm^{-1}) $\nu = 3313, 3148, 2985, 1617, 1537, 1501, 1413, 1343, 1257, 1217$.

3-(1H-Indol-5-yl)-1-(4-((1H-indol-5-yl)carbamoyl)amino)phenyl)urea (3). Pale brown solid (380 mg, yield: 45%), ^1H NMR (500 MHz, DMSO) δ 10.91 (s, 1H), 8.36 (d, $J = 40.2$ Hz, 2H), 7.66 (s, 1H), 7.31 (d, $J = 40.4$ Hz, 4H), 7.07 (s, 1H), 6.34 (s, 1H). $^{13}\text{C}\{^1\text{H}\}$ NMR (126 MHz, DMSO) δ : 153.2, 134.2, 132.2, 132.6, 127.7, 125.7, 118.8, 114.7, 111.2, 109.8, 100.9. Mp 317.0–323.4 $^{\circ}\text{C}$. IR (cm^{-1}) $\nu = 3315, 1614, 1559, 1505, 1474, 1406, 1309, 1220$.

3-(1H-Indol-5-yl)-1-(4-((1H-indol-5-yl)carbamothioyl)amino)phenyl)thiourea (4). Off-white solid (412 mg, yield: 92%), $R_f = 0.39$ (dichloromethane/MeOH = 95: 5). ^1H NMR (500 MHz, DMSO) δ 11.09 (s, 2H), 9.62 (s, 2H), 9.42 (s, 2H), 7.55 (s, 2H), 7.42 (s, 4H), 7.71–7.35 (m, 4H), 7.07 (dd, $J = 8.6, 2.0$ Hz, 2H), 6.43 (s, 2H). $^{13}\text{C}\{^1\text{H}\}$ NMR (126 MHz, DMSO) δ : 179.9, 136.1, 133.9, 130.6, 127.6, 126.1, 123.9, 119.5, 116.4, 111.3, 101.3. Mp 187.3–191.6 $^{\circ}\text{C}$. IR (cm^{-1}) $\nu = 3315, 1668, 1624, 1559, 1506, 1407, 1301, 1229, 1201$.

3-(1H-Indol-6-yl)-1-(4-((1H-indol-6-yl)carbamoyl)amino)phenyl)urea (5). Pale yellow color solid (364 mg, yield: 43%), ^1H NMR (500 MHz, DMSO) δ 10.89 (s, 1H), 8.49 (d, $J = 17.5$ Hz, 2H), 7.90–7.68 (m, 1H), 7.39 (d, $J = 8.4$ Hz, 1H), 7.36 (s, 2H), 7.25–7.14 (m, 1H), 6.84 (dd, $J = 8.5, 1.9$ Hz, 1H), 6.32 (s, 1H). $^{13}\text{C}\{^1\text{H}\}$ NMR (126 MHz, DMSO) δ : 153.4, 136.8, 134.7, 134.4, 124.8, 123.5, 120.4, 119.3, 112.4, 101.5, 101.3. Mp 329.5–336.3 $^{\circ}\text{C}$. IR (cm^{-1}) $\nu = 3299, 1630, 1589, 1552, 1509, 1454, 1402, 1345, 1324, 1295, 1220$.

3-(1H-Indol-6-yl)-1-(4-((1H-indol-6-yl)carbamothioyl)amino)phenyl)thiourea (6). Off-white solid (463 mg, yield: 100%), $R_f = 0.37$ (dichloromethane/MeOH = 95: 5). ^1H NMR (500 MHz, DMSO) δ 11.07 (s, 2H), 9.74 (s, 2H), 9.55 (s, 2H), 7.61 (s, 2H), 7.49 (d, $J = 8.4$ Hz, 2H), 7.44 (s, 4H), 7.32 (t, $J = 2.8$ Hz, 2H), 6.97 (dd, $J = 8.5, 1.9$ Hz, 2H), 6.40 (s, 2H). $^{13}\text{C}\{^1\text{H}\}$ NMR (126 MHz, DMSO) δ : 179.5, 136.0, 135.7,

132.8, 125.7, 125.2, 123.8, 119.8, 116.6, 107.2, 101.0. Mp 221.1–225.4 $^{\circ}\text{C}$. IR (cm^{-1}) $\nu = 3312, 1618, 1537, 1500, 1409, 1343, 1255, 1217$.

3-(1H-Indol-7-yl)-1-(4-((1H-indol-7-yl)carbamoyl)amino)phenyl)urea (7). Ash color solid (187 mg, yield: 44%), ^1H NMR (500 MHz, DMSO) δ 10.69 (s, 1H), 8.65 (s, 1H), 8.45 (s, 1H), 7.43 (s, 2H), 7.33 (t, $J = 2.8$ Hz, 1H), 7.30 (d, $J = 7.8$ Hz, 1H), 7.10 (d, $J = 7.6$ Hz, 1H), 6.94 (t, $J = 7.7$ Hz, 1H), 6.44 (dd, $J = 3.1, 1.9$ Hz, 1H). $^{13}\text{C}\{^1\text{H}\}$ NMR (126 MHz, DMSO) δ : 153.2, 134.2, 129.2, 128.4, 125.2, 123.9, 119.1, 119.0, 115.6, 113.4, 101.5. Mp < 360 $^{\circ}\text{C}$. IR (cm^{-1}) $\nu = 3397, 3275, 1634, 1572, 1537, 1504, 1435, 1343, 1236, 1206, 717, 661$.

3-(1H-Indol-7-yl)-1-(4-((1H-indol-7-yl)carbamothioyl)amino)phenyl)thiourea (8). Off-white solid (76 mg, yield: 42%), $R_f = 0.24$ (hexane/ethyl acetate = 7: 3). ^1H NMR (500 MHz, DMSO) δ 10.97 (s, 2H), 9.69 (s, 2H), 9.50 (s, 2H), 7.50 (s, 4H), 7.43 (d, $J = 7.7$ Hz, 2H), 7.31 (t, $J = 2.8$ Hz, 2H), 7.06 (d, $J = 8.0$ Hz, 1H), 6.98 (t, $J = 7.6$ Hz, 1H), 6.46 (dd, $J = 3.1, 1.9$ Hz, 1H). $^{13}\text{C}\{^1\text{H}\}$ NMR (126 MHz, DMSO) δ : 180.2, 136.0, 131.6, 129.4, 125.5, 123.9, 123.6, 118.8, 118.2, 109.2, 101.5. Mp 193.4–197.1 $^{\circ}\text{C}$. IR (cm^{-1}) $\nu = 3312, 3151, 1539, 1502, 1435, 1413, 1343, 1263, 1220, 744, 723$.

1-Phenyl-3-(4-((phenylcarbamoyl)amino)phenyl)urea (9). White solid (485 mg, yield: 93%), ^1H NMR (500 MHz, DMSO) δ 8.62 (s, 2H), 8.55 (s, 2H), 7.48–7.39 (m, 2H), 7.35 (s, 2H), 7.25 (dd, $J = 8.6, 7.3$ Hz, 2H), 7.00–6.87 (m, 1H). $^{13}\text{C}\{^1\text{H}\}$ NMR (126 MHz, DMSO) δ : 152.6, 139.9, 134.1, 128.7, 121.6, 119.0, 118.1. Mp < 360 $^{\circ}\text{C}$. IR (cm^{-1}) $\nu = 3296, 2985, 1628, 1592, 1548, 1506, 1445, 1403, 1295, 1223, 729, 693$.

1-Phenyl-3-(4-((phenylcarbamothioyl)amino)phenyl)thiourea (10). White solid (514 mg, yield: 91%), $R_f = 0.56$ (dichloromethane/MeOH = 95: 5). ^1H NMR (500 MHz, DMSO) δ 9.77 (d, $J = 4.7$ Hz, 4H), 7.50–7.48 (m, 4H), 7.45 (s, 4H), 7.33 (dd, $J = 8.5, 7.4$ Hz, 2H), 7.15–7.06 (m, 2H). $^{13}\text{C}\{^1\text{H}\}$ NMR (126 MHz, DMSO) δ 189.5, 139.5, 135.8, 128.4, 123.8,

123.6, 123.5. Mp < 360 °C. IR (cm⁻¹) ν = 3195, 3200, 1536, 1495, 1337, 1255, 1217, 1021, 746. Physical and spectral data were in agreement with the literature.²⁴

Chemical and Peptide Source. Thioflavin-T (ThT) was purchased from Alfa Aesar (Ward Hill, MA) for the -syn ThT assays and Sigma-Aldrich (St. Louis, MO) for the tau 0N3R ThT assays. Heparin sodium salt was purchased from Millipore-Sigma. Recombinant α -syn and tau 2N4R was purchased from rPeptide (Watkinsville, GA). The recombinant p-tau isoform 1N4R was prepared as published previously.^{25–27} For expression and purification of tau 0N4R, a bacterial expression plasmid consisting of the vector pET30a carrying a cDNA encoding the human Tau 0N4R isoform was a kind gift from Dr. Benjamin Wolozin (Boston University). *Escherichia coli* stock (Rosetta BL21 Ecoli (CamR) containing pET30a[0N4R tau wt] (KanR)) were grown in LB media supplemented with kanamycin (50 μ g/mL) and chloramphenicol (50 μ g/mL). Protein overexpression was induced by the addition of 1 mM IPTG for ~18 h at 37 °C, and cells were pelleted by centrifugation at 6000g for 15 min at 4 °C. The cells were resuspended in lysis buffer (10 mM Hepes pH 7.4, 50 mM NaCl, 1 mM MgCl₂, 1 mM PMSF, 1 \times PIC, 0.5 mM DTT) and lysed by sonication at 30 s On 1 min Off at ca. 30–45% power for ca. 3–5 min. Lysate was centrifuged at 10,000g for 10 min at 4 °C and supernatant was transferred with 7.8 mL (total) of 3 M NaCl. The lysate was incubated for 10 min in an 80 °C water bath and then cooled for 10 min in an ice bath. The lysate was centrifuged at 10,000g, 4 °C for 10 min, and the supernatant was transferred to new tubes. The supernatant was dialyzed overnight against cation exchange buffer (50 mM MES, 1 M NaCl, 1 mM DTT, pH 6.0). The dialysate was loaded onto a HiPrep SP HP column, and proteins were eluted with a linear gradient ranging from 50 mM to 1 M NaCl. Fractions containing tau isoform 0N4R were pooled, and the resulting protein solution was dialyzed against PBS (pH 7.4) and stored at -80 °C.

0N3R Expression and Purification. 0N3R expression and purification were done as described previously.^{28–30} The pET-47b(+) vector containing the gene for 0N3R was transformed to BL21 (DE3). A starter culture grown overnight was inoculated into terrific broth media supplemented with kanamycin (50 μ g/mL), which was then grown at 37 °C with shaking at 200 rpm. Protein overexpression was induced at an OD₆₀₀ of 0.6–0.8 using 0.1 mM IPTG for 3–4 h at 37 °C.

Cells from the expression were resuspended in lysis buffer (25 mM Na₃PO₄, 300 mM NaCl, 5 mM imidazole, 1 mM DTT, and 1 mM PMSF) at pH 7.4. Resuspended cells were lysed via sonication at 30 s On and 10 s Off for 10 min at 60% power. Cell lysate was centrifuged at 100,000g. 0N3R was purified from the supernatant using Ni-NTA. The elute from Ni-NTA was dialyzed to remove imidazole. Afterward, the His-tag was cleaved off using human rhinovirus (HRV) 3C protease by incubating it with 0N3R at a 1:100 molar ratio for 4 h at 4 °C, and an additional Ni-NTA column was performed to isolate His-tag-free 0N3R. The Ni-NTA fraction containing His-tag-free 0N3R was dialyzed against a salt-free buffer prior to further purification.

0N3R was purified with HiTrap SP Sepharose FF cation exchange column using 50 mM Tris at pH 7.4 and 50 mM Tris, 1 M NaCl at pH 7.4 as Buffer A and Buffer B, respectively. Fractions containing 0N3R were buffer exchanged into 50 mM Tris 25 mM NaCl pH 7.4 using a PD10 desalting column and stored at -80 °C until use. All buffers in this step were treated with 1 g of CHELEX beads per 1 L of buffer overnight.

HRV3C Expression and Purification. The plasmid employed for HRV3C was procured from Addgene.³¹ Transformed BL21 (DE3) bacterial cells were cultivated until they reached an OD₆₀₀ of 0.8, at which point they were induced with 0.1 mM IPTG. Induction was carried out at a lowered temperature of 16 °C and continued for 16 h. Subsequently, the cultivated cells were harvested and the cellular integrity was disrupted via sonication. The resulting cell lysate was subjected to high-speed centrifugation at 100,000g. HRV3C protease was subsequently extracted from the supernatant employing Ni-NTA affinity chromatography and further subjected to purification through a HiPrep 16/60 Sephacryl S-100 HR size exclusion column.

Fractions containing HRV3C were carefully collected and preserved with a 10% glycerol additive at -80 °C, awaiting subsequent utilization.

Thioflavin Fluorescence Assays. Thioflavin fluorescence assays were used to monitor fibril formation of commercial recombinant α -syn at a final concentration of 6 μ M and treated with control DMSO and different compounds. The recombinant α -syn obtained from rPeptide was validated with proper quality control to confirm the monomeric state of the protein. Kinetics of fibril formation have been performed using thioflavin T (ThT) as published previously.^{7,13,14,25} Briefly, ThT was used at a final concentration of 20 μ M. α -Syn was dissolved in 20 mM Tris-HCl (pH 7.4) supplemented with 100 mM NaCl to a stock solution of 280 μ M prior to resuspension in a ThT buffer to obtain a final concentration of 6 μ M (in each well). Compounds and ThT were first added to the wells. The kinetics of fibril formation begin when the α -syn is solubilized in the ThT buffer (10 mM PBS (pH 7.4), supplemented with 0.5 mM SDS and 300 mM NaCl) and added to a nontreated black 96-well microplate with a transparent flat bottom. Each well was filled with a maximum volume of 150 μ L of buffer with one 3 mm borosilicate bead. The background fluorescence signal consisted of ThT in a buffer and 0.25% DMSO without α -syn. The excitation and emission wavelengths consisted of 440 and 485 nm, respectively. Measurements were acquired with Synergy HT multimode microplate reader (BioTek, Winooski, VT) and taken at 37 °C every 20 min with 10 s shaking prior to reading the plate. Kinetics were monitored for 40 to 50 h. Samples were measured in three to five replicates. The experiments were repeated two additional times using different α -syn stock solutions and a final concentration of 2 μ M. For each time point, arbitrary units of fluorescence were calculated from the mean values normalized against the maximum value. The percentage of fluorescence intensity at the plateau phase in Table 1 was expressed as mean \pm SEM. Concerning the dose-response curve depicted in Figure 2, the data were plotted using GraphPad Prism.

Concerning the tau (isoform 0N3R) kinetics of fibril formation, measurements of ThT fluorescence were performed with a solution of the protein diluted to a final concentration of 10 μ M in CHELEX-treated 50 mM Tris, 25 mM NaCl (pH 7.4) supplemented with 2.5 μ M heparin, 30 μ M ThT, 1 mM dithiothreitol (DTT), 1 mM 4-(2-aminoethyl)benzenesulfonyl fluoride hydrochloride, and 100 μ M compound. The aggregation reaction (200 μ L each) was pipetted into the wells of a 96-well plate. The positive control consisted of Tau 0N3R without compound treatment. The background (BG) signal was obtained with all components in the absence of heparin. The plate was incubated at 37 °C with interval shaking at 200 rpm in a Biotek Synergy plate reader. ThT fluorescence

was measured every 5 min with excitation and emission wavelengths of 440 and 480 nm, and the data were plotted using BioTek Gen5 software. All reactants used in the aggregation reactions were filtered through a 0.2 μm filter.

AFM Imaging. AFM images of the tau aggregates were acquired in accordance with previously established protocols.^{32–34} To prepare the 0N3R aggregates, we followed the procedures employed in Thioflavin T (ThT) fluorescence assays with the exclusion of ThT dye. At the 47 h time point, the aggregation solution underwent a 1:50 dilution, and subsequently, a 20 μL aliquot of the diluted solution was carefully deposited onto a freshly cleaved mica substrate. Any loosely adhered 0N3R aggregates were removed by gentle blotting and subsequent washing with 0.2 μm of filtered Milli-Q water. Following these preparation steps, the samples were allowed to air-dry and were immediately subjected to imaging using a Veeco-Multimode Atomic Force Microscope (AFM) in tapping mode.

For imaging, an aluminum-coated cantilever with a force constant of 2.8 N/m and a resonance frequency of 75 kHz was employed. Image acquisition was conducted at two distinct sizes: 10 \times 10 μm^2 and 3.33 \times 3.33 μm^2 , with scanning rates of approximately 0.6 and 1.0 Hz, respectively. Notably, the reported images were obtained at a resolution of 1024 lines per sample. Subsequently, the acquired images underwent postprocessing using Gwyddion³⁵ software, and the dimensions, encompassing both lengths and heights, of the 0N3R tau fibers were quantified employing the FiberApp³⁶ analysis tool.

Disaggregation Experiments. α -Syn was incubated at 37 $^\circ\text{C}$ for 2 days at a final concentration of 9.4 μM in 10 mM PBS (pH 7.4), supplemented with 0.5 mM SDS and 300 mM NaCl. ThT was performed as indicated in the [Experimental Section](#) with ThT and compound added at 20 and 100 μM , respectively. After 40 h, samples were collected and evaluated with TEM. Conditions were performed 3 to 6 times. Experiments were repeated twice. For each assay, the final concentration of α -syn was 6 μM .

Photoinduced Cross-Linking of Unmodified Proteins (PICUP) Assay. To induce oligomerization by cross-linking, α -syn (from rPeptide, LLC) was diluted in 10 mM phosphate buffer (pH 7.4) to reach a final concentration of 30 or 50 μM . Concerning tau (0N4R and 2N4R) and p-tau (1N4R), the final concentration consisted of 6 μM . Different compounds were added to the protein solution at a final concentration of 50 μM . PICUP assays were performed with the following controls: samples without light exposure, without Ru(bpy) or ammonium persulfate, and without compound (i.e., 0.125% DMSO). The addition of 2 μL of Ru(bpy) (300 μM final concentration) and 2 μL ammonium persulfate (6 mM final concentration) to the samples is required prior to light exposition.^{7,13,14} Light exposure was of a 1 s (α -syn), 2 min (tau 0N4R, p-tau 1N4R), or 4 min (tau 2N4R) duration with a 53 W (120 V) incandescent lamp installed in a homemade dark-box. Each tube contained a final volume of 20 μL . To end the radical reaction, 8.3 μL of Laemmli loading buffer containing 15% β -mercaptoethanol was added to the protein solution, and the mixture was subjected to incubation at 95 $^\circ\text{C}$ for 10 min. The cross-linked α -syn and tau samples were separated by using a 16% SDS-PAGE gel and then stained with Coomassie blue staining. Most PICUP experiments were repeated 2 to 3 times.

Transmission Electron Microscopy (TEM). TEM was utilized to detect fibril formation at the end of ThT kinetics of fibril formation as mentioned in previous publication.^{7,13,14} A

volume of 10 μL was applied on a 400-mesh Formvar carbon-coated copper grid (Electron Microscopy Sciences, Hatfield, PA). The grids were incubated in contact with α -syn samples for 1 min. Grids were washed three times with distilled water. They were carefully air-dried and incubated for 1 min in a fresh solution of 1% uranyl acetate. After removal of excess stain, acquisition of pictures was performed with the following settings using a transmission electron microscope (JEOL 1400 Flash, Japan): accelerating voltage of 100 kV and magnification of 40k.

Far-UV CD Analyses on the Structural Effects of Compounds on α -Synuclein Aggregation. CD spectra of the secondary structure of α -syn samples were recorded at 25 $^\circ\text{C}$ under a constant flow of N_2 using a JASCO-810 spectropolarimeter (Jasco, Easton, MD). Spectra were recorded over a wavelength range of 200–260 nm using a quartz cuvette of 1 mm path length and an instrument scanning speed of 100 nm/min, with a response time of 2 s and a bandwidth of 1 nm. All α -syn samples were dissolved to a final concentration of 12 μM in 10 mM PBS (pH 7.4) containing 300 mM NaCl and 0.5 mM SDS.

Prior to CD analyses, 100 μM compounds **1** and **2** as well as curcumin (positive control, obtained from Indofine Chemical Company, Inc., Hillsborough, NJ) and 0.25% DMSO were incubated with 12 μM α -syn in the buffer at 37 $^\circ\text{C}$ for 0, 24, and 48 h. 0.25% DMSO with buffer alone (no α -syn) was used as the baseline and subtracted from subsequent readings of all samples. Each result is given as the average of 5 scans taken of three measurements at room temperature. The data were converted to mean residue ellipticity (θ) and analyzed using the software CDPro. All CD spectra were averaged and baseline-corrected for signal contributions due to the buffer.

α -Syn utilized for the CD analyses was freshly prepared in our laboratory as the following. The α -syn plasmid was obtained as a gift from Dr. Lisa Lapidus (Department of Physics and Astronomy, Michigan State University). The PUC19/18 α -syn plasmid that carries human α -syn cDNA was transformed into competent cells (Rosetta BL21) on ampicillin-coated agar plates. A colony was used for a small bacteria culture (10 mL of LB medium supplemented with 50 $\mu\text{g}/\text{mL}$ ampicillin) and then left to shake overnight at 37 $^\circ\text{C}$. The small culture was transferred to a 1 L culture of *E. coli* and grown for 3 h with shaking. The expression of the protein was induced with the addition of 1 mM IPTG after the larger culture reached an OD₆₀₀ 0.5–0.7. After 6 h, cells were centrifuged to obtain the pellet at 6600g for 15 min at 4 $^\circ\text{C}$ and then resuspended in lysis buffer (10 mM Tris pH 7.6, 750 mM NaCl, 1 mM EDTA with protease inhibitor). The lysates were subjected to sonication for 5 min (30 s On, 30 s Off pulses at 30–45% power) and boiled at 95 $^\circ\text{C}$ for 15 min. The boiled sample was then centrifuged at 6600g for 15 min at 4 $^\circ\text{C}$, and the supernatant obtained was transferred to a new tube, followed by overnight dialysis with 10 mM TRIS pH 7.6, 1 mM EDTA. The dialyzed supernatant was purified by anion exchange chromatography (HiTrap Q HP 16/10) using a mobile phase of 25 mM Tris pH 7.6 and a linear gradient of 20 column volumes of elution buffer to 1 M NaCl. Fractions with α -syn were pooled and concentrated. The concentrated fraction was stored at -80 $^\circ\text{C}$. Similar CD data were obtained with the α -syn obtained commercially from rPeptide using a concentration of 6 μM .

α -Syn (or αS) Inclusion-Forming Neuroblastoma Cell Experiment. Dox-inducible neuroblastoma cells M17D-TR/ αS -3K::YFP have been used previously.²² 96-well plates were used with a cellular density of 30,000 cells per well. Compounds

were added after 24 h, and α S-3K::YFP transgene expression was induced 48 h later. Induction was performed by adding 1 μ g per mL (final concentration) dox to culture media. Cells were incubated in the Incucyte Zoom 2000 platform (Essen Biosciences), and images (green, bright field) were taken continuously. End point analysis of inclusion formation or growth was performed 48 h after induction (96 h after plating). The Incucyte processing definition "Inclusions" was created as follows: Parameters, Fixed Threshold, Threshold (GCU) 50; Edge Split On, Edge Sensitivity 100; Cleanup, Hole Fill (μm^2): 10, Adjust Size (pixels): 0; Filters, Area (μm^2): max 50, Mean Intensity: min 60, Integrated Intensity: min 2000. Cell confluence was measured by the processing definition 'Cells': Parameters, Segmentation Adjustment 0.7; Cleanup, all parameters set to 0; Filters, Area (μm^2): min 345.00.

Docking Studies. The ligand geometries were optimized using Becke's three-parameter hybrid exchange functional along with the Lee–Yang–Parr correction functional (B3LYP) method in conjunction with the 6-311G+(d,p) basis set using Gaussian 16 software package (Tables S1 and S2). The molecular docking was performed with AutoDock 4.0 (Version 1.5.7). The grid size was set to 100 \times 100 \times 100 points with a grid spacing of 0.375 Å to cover the reported active site (Val3, Lys10, Ala17, Lys21, Ala69, Val70, Gly73, Ala76, Val77, Lys80, Glu83, Gly84, Ser87) of human α -synuclein protein (PDB ID: 1XQ8) containing 140 amino acids.³⁷ The intermolecular polar interactions and bond angles were analyzed and visualized by UCSF Chimera (version 1.14).

■ ASSOCIATED CONTENT

Data Availability Statement

The data underlying this study are available in the published article and its [Supporting Information](#).

SI Supporting Information

The Supporting Information is available free of charge at <https://pubs.acs.org/doi/10.1021/acsomega.3c07453>.

Data pertaining to the characterization of compounds (NMR, HRMS, IR), fibril measurement results by AFM, cytotoxicity determination of compounds 1 and 2 with neuroblastoma cells (crystal violet, MTT), structural analyses with circular dichroism, and additional diurea compounds and their α -syn antifibrillary effects with chemical structure characterization of each additional compound (PDF)

■ AUTHOR INFORMATION

Corresponding Author

Jessica S. Fortin – Department of Basic Medical Sciences, College of Veterinary Medicine, Purdue University, West Lafayette, Indiana 47907, United States; orcid.org/0000-0002-1007-9360; Email: fortinj@purdue.edu

Authors

Susantha K. Ganegamage – Department of Basic Medical Sciences, College of Veterinary Medicine, Purdue University, West Lafayette, Indiana 47907, United States

Eduardo Ramirez – Department of Basic Medical Sciences, College of Veterinary Medicine, Purdue University, West Lafayette, Indiana 47907, United States; orcid.org/0000-0002-3079-3844

Heba Alnakhala – Ann Romney Center for Neurologic Diseases, Department of Neurology, Brigham and Women's Hospital

and Harvard Medical School, Boston, Massachusetts 02115, United States

Arati Tripathi – Ann Romney Center for Neurologic Diseases, Department of Neurology, Brigham and Women's Hospital and Harvard Medical School, Boston, Massachusetts 02115, United States

Cuong Calvin Duc Nguyen – Department of Chemistry, College of Sciences, Purdue University, West Lafayette, Indiana 47907, United States

Ashique Zami – Purdue Institute for Inflammation, Immunology and Infectious Disease, Purdue University, West Lafayette, Indiana 47907, United States

Raluca Ostafe – Purdue Institute for Inflammation, Immunology and Infectious Disease, Purdue University, West Lafayette, Indiana 47907, United States

Shiliang Tian – Department of Chemistry, College of Sciences, Purdue University, West Lafayette, Indiana 47907, United States

Ulf Dettmer – Ann Romney Center for Neurologic Diseases, Department of Neurology, Brigham and Women's Hospital and Harvard Medical School, Boston, Massachusetts 02115, United States

Complete contact information is available at:

<https://pubs.acs.org/10.1021/acsomega.3c07453>

Author Contributions

This project was conceived by J.S.F. Synthesis and characterization of compounds were performed by S.K.G. The ThT assays, cross-linking assays, and data interpretation were performed by E.R. TEM analyses and cytotoxicity assays (Supporting Information) were performed by J.S.F. Tau ThT and AFM experiments were conducted by C.D.C.N. Protein procurement was done with A.Z., R.O., C.D.C.N., and T.S. The cell culture experiments, statistics, and data interpretation were conducted by H.A., A.T., and U.D. Results were discussed with J.S.F., S.K.G., E.R., C.D.C.N., R.O., T.S., and U.D. The manuscript was drafted by S.K.G. and J.S.F. followed by editorial work from S.K.G., E.R., R.O., C.D.C.N., T.S., U.D., and J.S.F. All authors contributed to this manuscript and approved the final version of this manuscript.

Funding

J.S.F. support was provided by the National Institutes of Health (NIH) grants (AG070447, AG071985). U.D. was supported by NIH grants NS121826 and NS099328.

Notes

The authors declare no competing financial interest.

■ ACKNOWLEDGMENTS

The authors acknowledge the professional services of Alicia Withrow at the Center for Advanced Microscopy at Michigan State University. They thank Min-Hao Kuo (Michigan State University), Lisa J. Lapidus (Michigan State University), and Bejamin Wolozin (Boston University) for providing the constructs for the production of p-tau (1N4R), α -syn, and tau isoform 0N4R, respectively. The authors are grateful to Babak Borhan (Chemistry Department, Michigan State University) for providing them access to circular dichroism. This work was supported in part (i.e., for the AFM) by the Research Instrument Center in the Department of Chemistry at Purdue University.

ABBREVIATIONS

A β , amyloid- β ; AD, Alzheimer's disease; dox, doxycycline; CD, circular dichroism; PD, Parkinson's disease; PICUPs, photo-induced cross-linking of unmodified proteins; RPD, relative pixel density; SEM, standard error of the mean; α -syn, α -synuclein; TEM, transmission electron microscopy; ThT, thioflavin T

REFERENCES

- (1) Marras, C.; Beck, J. C.; Bower, J. H.; Roberts, E.; Ritz, B.; Ross, G. W.; Abbott, R. D.; Savica, R.; Van Den Eeden, S. K.; Willis, A. W.; Tanner, C. Prevalence of Parkinson's disease across North America. *NPJ Parkinson's Dis.* **2018**, *4*, 21.
- (2) Shahmoradian, S. H.; Lewis, A. J.; Genoud, C.; Hench, J.; Moors, T. E.; Navarro, P. P.; Castano-Diez, D.; Schweighauser, G.; Graff-Meyer, A.; Goldie, K. N.; et al. Lewy pathology in Parkinson's disease consists of crowded organelles and lipid membranes. *Nat. Neurosci.* **2019**, *22* (7), 1099–1109.
- (3) Cardinale, A.; Calabrese, V.; de Iure, A.; Picconi, B. Alpha-Synuclein as a Prominent Actor in the Inflammatory Synaptopathy of Parkinson's Disease. *Int. J. Mol. Sci.* **2021**, *22* (12), No. 6517.
- (4) Mahul-Mellier, A. L.; Burtscher, J.; Maharjan, N.; Weerens, L.; Croisier, M.; Kuttler, F.; Leleu, M.; Knott, G. W.; Lashuel, H. A. The process of Lewy body formation, rather than simply alpha-synuclein fibrillization, is one of the major drivers of neurodegeneration. *Proc. Natl. Acad. Sci. U.S.A.* **2020**, *117* (9), 4971–4982.
- (5) Winner, B.; Jappelli, R.; Maji, S. K.; Desplats, P. A.; Boyer, L.; Aigner, S.; Hetzer, C.; Loher, T.; Vilar, M.; Campioni, S.; et al. In vivo demonstration that alpha-synuclein oligomers are toxic. *Proc. Natl. Acad. Sci. U.S.A.* **2011**, *108* (10), 4194–4199.
- (6) Robustelli, P.; Ibanez-de-Opakua, A.; Campbell-Bezatz, C.; Giordanetto, F.; Becker, S.; Zweckstetter, M.; Pan, A. C.; Shaw, D. E. Molecular Basis of Small-Molecule Binding to alpha-Synuclein. *J. Am. Chem. Soc.* **2022**, *144* (6), 2501–2510.
- (7) Fortin, J. S.; Shimanaka, K.; Saraswati, A. P.; Liu, M.; Wang, K. W.; Hagar, H. T.; Maity, S.; Ganegamage, S. K.; Ellsworth, E.; Counts, S. E.; et al. Anti-fibrillization effects of sulfonamide derivatives on alpha-synuclein and hyperphosphorylated tau isoform 1N4R. *J. Mol. Struct.* **2022**, *1267*, No. 133574.
- (8) Kurnik, M.; Sahin, C.; Andersen, C. B.; Lorenzen, N.; Giehm, L.; Mohammad-Beigi, H.; Jessen, C. M.; Pedersen, J. S.; Christiansen, G.; Petersen, S. V.; et al. Potent alpha-Synuclein Aggregation Inhibitors, Identified by High-Throughput Screening, Mainly Target the Monomeric State. *Cell Chem. Biol.* **2018**, *25* (11), 1389–1402.
- (9) Vittorio, S.; Adornato, I.; Gitto, R.; Pena-Diaz, S.; Ventura, S.; De Luca, L. Rational design of small molecules able to inhibit alpha-synuclein amyloid aggregation for the treatment of Parkinson's disease. *J. Enzyme Inhib. Med. Chem.* **2020**, *35* (1), 1727–1735.
- (10) Ross, N. T.; Metkar, S. R.; Le, H.; Burbank, J.; Cahill, C.; Germain, A.; MacPherson, L.; Bittker, J.; Palmer, M.; Rogers, J. et al. Identification of a Small Molecule that Selectively Inhibits alpha-Synuclein Translational Expression. In *Probe Reports from the NIH Molecular Libraries Program*; NIH, 2010.
- (11) Fortin, J. S.; Benoit-Biancamano, M. O.; Gaudreault, R. C. Discovery of ethyl urea derivatives as inhibitors of islet amyloid polypeptide fibrillization and cytotoxicity. *Can. J. Physiol. Pharmacol.* **2016**, *94* (3), 341–346.
- (12) Maity, S.; Shimanaka, K.; Rivet, L. N.; O'Dell, M.; Rashid, A. M.; Isa, N. B. M.; Kepczynski, R. S.; Dettmer, U.; Borhan, B.; Fortin, J. S. In vitro characterization of urea derivatives to inhibit alpha-synuclein early-stage aggregation. *J. Mol. Struct.* **2022**, *1249*, No. 131569.
- (13) Ramirez, E.; Ganegamage, S. K.; Elbatrawy, A. A.; Alnakhala, H.; Shimanaka, K.; Tripathi, A.; Min, S.; Rochet, J. C.; Dettmer, J.-C. R. U.; Dettmer, U.; Fortin, J. S. 5-Nitro-1,2-benzothiazol-3-amine and N-Ethyl-1-[(ethylcarbamoyl)(5-nitro-1,2-benzothiazol-3-yl)amino]-formamide Modulate α -Synuclein and Tau Aggregation. *ACS Omega* **2023**, *8*, 20102–20115, DOI: 10.1021/acsomega.3c02668.
- (14) Ramirez, E.; Min, S.; Ganegamage, S. K.; Shimanaka, K.; Sosa, M. G.; Dettmer, U.; Rochet, J.-C.; Fortin, J. S. Discovery of 4-aminoindoole carboxamide derivatives to curtail alpha-synuclein and tau isoform 2N4R oligomer formation. *Results Chem.* **2023**, *5*, No. 100938.
- (15) Adeyomoye, O. I.; Akintayo, C. O.; Omotuyi, K. P.; Adewumi, A. N. The Biological Roles of Urea: A Review of Preclinical Studies. *Indian J Nephrol* **2022**, *32* (6), 539–545.
- (16) Jahan, I.; Nayeem, S. M. Effect of Urea, Arginine, and Ethanol Concentration on Aggregation of (179)CVNITV(184) Fragment of Sheep Prion Protein. *ACS Omega* **2018**, *3* (9), 11727–11741.
- (17) Bhat, M. Y.; Mir, I. A.; Ul Hussain, M.; Singh, L. R.; Dar, T. A. Urea ameliorates trimethylamine N-oxide-Induced aggregation of intrinsically disordered alpha-casein protein: the other side of the urea-methylamine counteraction. *J. Biomol. Struct. Dyn.* **2023**, *41* (8), 3659–3666.
- (18) Rabilloud, T. Detergents and chaotropes for protein solubilization before two-dimensional electrophoresis. *Methods Mol. Biol.* **2009**, *528*, 259–267.
- (19) Fu, Y.; Zhao, J.; Chen, Z. Insights into the Molecular Mechanisms of Protein-Ligand Interactions by Molecular Docking and Molecular Dynamics Simulation: A Case of Oligopeptide Binding Protein. *Comput. Math. Methods Med.* **2018**, *2018*, No. 3502514.
- (20) Lippert, T.; Rarey, M. Fast automated placement of polar hydrogen atoms in protein-ligand complexes. *J. Cheminf.* **2009**, *1* (1), No. 13.
- (21) Maltarollo, V. G.; Honorio, K. M. Ligand- and structure-based drug design strategies and PPARdelta/alpha selectivity. *Chem. Biol. Drug Des.* **2012**, *80* (4), 533–544.
- (22) Terry-Kantor, E.; Tripathi, A.; Imberdis, T.; LaVoie, Z. M.; Ho, G. P. H.; Selkoe, D.; Fanning, S.; Ramalingam, N.; Dettmer, U. Rapid Alpha-Synuclein Toxicity in a Neural Cell Model and Its Rescue by a Stearoyl-CoA Desaturase Inhibitor. *Int. J. Mol. Sci.* **2020**, *21* (15), No. 5193.
- (23) Imberdis, T.; Negri, J.; Ramalingam, N.; Terry-Kantor, E.; Ho, G. P. H.; Fanning, S.; Stirtz, G.; Kim, T. E.; Levy, O. A.; Young-Pearse, T. L.; et al. Cell models of lipid-rich alpha-synuclein aggregation validate known modifiers of alpha-synuclein biology and identify stearoyl-CoA desaturase. *Proc. Natl. Acad. Sci. U.S.A.* **2019**, *116* (41), 20760–20769.
- (24) Hara, M.; Minagawa, K.; Imada, Y.; Arakawa, Y. Synthesis of Optically Active Polyguanidines by Polyaddition Reaction of Biscarbodiimides with Chiral Diamines. *ACS Omega* **2021**, *6* (48), 33215–33223.
- (25) Fortin, J. S.; Hetak, A. A.; Duggan, K. E.; Burglass, C. M.; Penticoff, H. B.; Schott, H. C., 2nd Equine pituitary pars intermedia dysfunction: a spontaneous model of synucleinopathy. *Sci. Rep.* **2021**, *11* (1), No. 16036.
- (26) Sui, D.; Xu, X.; Ye, X.; Liu, M.; Miannecki, M.; Rattanasinchai, C.; Buehl, C.; Deng, X.; Kuo, M. H. Protein interaction module-assisted function X (PIMAX) approach to producing challenging proteins including hyperphosphorylated tau and active CDK5/p25 kinase complex. *Mol. Cell. Proteomics* **2015**, *14* (1), 251–262.
- (27) Liu, M.; Sui, D.; Dexheimer, T.; Hovde, S.; Deng, X.; Wang, K. W.; Lin, H. L.; Chien, H. T.; Kweon, H. K.; Kuo, N. S.; et al. Hyperphosphorylation Renders Tau Prone to Aggregate and to Cause Cell Death. *Mol. Neurobiol.* **2020**, *57* (11), 4704–4719.
- (28) Dregni, A. J.; Wang, H. K.; Wu, H.; Duan, P.; Jin, J.; DeGrado, W. F.; Hong, M. Inclusion of the C-Terminal Domain in the beta-Sheet Core of Heparin-Fibrillized Three-Repeat Tau Protein Revealed by Solid-State Nuclear Magnetic Resonance Spectroscopy. *J. Am. Chem. Soc.* **2021**, *143* (20), 7839–7851.
- (29) Barghorn, S.; Biernat, J.; Mandelkow, E. Purification of recombinant tau protein and preparation of Alzheimer-paired helical filaments in vitro. *Methods Mol. Biol.* **2005**, *299*, 35–51.
- (30) Wu, L.; Wang, Z.; Lad, S.; Gilyazova, N.; Dougharty, D. T.; Marcus, M.; Henderson, F.; Ray, W. K.; Siedlak, S.; Li, J.; et al. Selective Detection of Misfolded Tau From Postmortem Alzheimer's Disease Brains. *Front. Aging Neurosci.* **2022**, *14*, No. 945875.

- (31) Abdelkader, E. H.; Otting, G. NT*-HRV3CP: An optimized construct of human rhinovirus 14 3C protease for high-yield expression and fast affinity-tag cleavage. *J. Biotechnol.* **2021**, *325*, 145–151.
- (32) Lyu, C.; Da Vela, S.; Al-Hilaly, Y.; Marshall, K. E.; Thorogate, R.; Svergun, D.; Serpell, L. C.; Pastore, A.; Hanger, D. P. The Disease Associated Tau35 Fragment has an Increased Propensity to Aggregate Compared to Full-Length Tau. *Front. Mol. Biosci.* **2021**, *8*, No. 779240.
- (33) Wegmann, S.; Muller, D. J.; Mandelkow, E. Investigating fibrillar aggregates of Tau protein by atomic force microscopy. *Methods Mol. Biol.* **2012**, *849*, 169–183.
- (34) Makky, A.; Bousset, L.; Madiona, K.; Melki, R. Atomic Force Microscopy Imaging and Nanomechanical Properties of Six Tau Isoform Assemblies. *Biophys. J.* **2020**, *119* (12), 2497–2507.
- (35) Necas, D.; Klapetek, P. Gwyddion: an open-source software for SPM data analysis. *Cent. Eur. J. Phys.* **2012**, *10* (1), 181–188.
- (36) Usov, I.; Mezzenga, R. FiberApp: An Open-Source Software for Tracking and Analyzing Polymers, Filaments, Biomacromolecules, and Fibrous Objects. *Macromolecules* **2015**, *48* (5), 1269–1280.
- (37) Selvaraj, S.; Sundar, S.; Piramanayagam, S. A Computational Approach towards Targeting Parkinson's Disease: The Discovery of Potential Inhibitors against Alpha-Synuclein and Pten-Induced Putative Kinase 1 Protein *Molecular Biology: Open Access* **2021**, *102* 7.